Hindawi
Advances in Materials Science and Engineering
Volume 2022, Article ID 5168629, 9 pages
https://doi.org/10.1155/2022/5168629

Research Article

Influence of Microalloying Process on Dynamic Mechanical Relaxation of ZrCo-Based Amorphous Alloy

Rosario Mireya Romero Parra,[1] Indrajit Patra,[2] Fatima Safaa Fahim,[3] Samar Emad Izzat,[4] Ali Thaeer Hammid,[5] and Saeed Razavinejad[6]

[1]*Department of General Studies, Universidad Continental, Lima, Peru*
[2]*NIT Durgapur, Durgapur, West Bengal, India*
[3]*Anesthesia Techniques Department, Al-Mustaqbal University College, Babylon, Iraq*
[4]*Pharmacy Department, Al-Nisour University College, Baghdad, Iraq*
[5]*Computer Engineering Techniques Department, Faculty of Information Technology, Imam Ja'afar Al-Sadiq University, Baghdad, Iraq*
[6]*Department of Mechanical Engineering, Islamic Azad University, Isfahan, Iran*

Correspondence should be addressed to Saeed Razavinejad; saeedrazavinejad.ac@gmail.com

Received 27 May 2022; Revised 1 August 2022; Accepted 8 August 2022; Published 13 September 2022

Academic Editor: Majid Samavatian

In this study, the dynamic mechanical spectroscopy was used to characterize the effects of minor Ni addition on the relaxation behavior of ZrCoAl bulk metallic glass (BMG). For this purpose, the Kohlrausch–Williams–Watts (KWW) function and quasi-point defect (QPD) model were used for evaluation of relaxation under the different aging temperatures. The results indicated that the Ni addition shifted the relaxation process to the higher temperatures. Moreover, the estimations showed that the activation energy of relaxation was 5.951 eV and 6.205 eV for ZrCoAl and ZrCoAlNi, respectively. It was also revealed that the microalloying process enhanced the structural defects in the system and led to the improvement of dynamic heterogeneity in the BMG. Comparing the physical models, it is suggested that a small change in the structural defects intensifies the dynamic heterogeneity in the material.

1. Introduction

Owing to their amorphous structure, bulk metallic glasses (BMGs) exhibit unique rheological and mechanical properties, opening up many possibilities to apply them in advanced engineering systems [1–4]. However, despite their crystalline counterparts, BMGs show complex relaxation behaviors making it necessary to precisely evaluate their glassy microstructure [5–8]. Among several techniques, dynamic mechanical analysis (DMA) is one of the efficient methods for identification and study of mechanical relaxation in the glassy alloys [9–12]. The studies indicated that the mechanical spectroscopy can reveal the dynamic relaxation of BMGs under different states such as rejuvenation, annealing, thermal variations, and compositional changes [13–16]. Among them, the role of minor addition on the dynamic relaxation of amorphous alloys can be easily analyzed through the DMA experiment [17–19]. To provide some examples, Tao et al. [20] indicated that the minor addition of Dy into the ZrCuAl BMG improved the structural heterogeneity and intensified the dynamic relaxation in the glassy system. Raya et al. [21] applied DMA to conduct strain-rate jump test for ZrCoAl(Si) BMGs. Their results demonstrated that the Si microalloying process weakened the sensitivity of amorphous alloy to the flow stresses and enhanced the structural stability under the rise of temperature and strain rate. Using the DMA method, Xu et al. [22] found that the addition of 10 at.% Nb into the CuZr glassy alloy improved the relaxation enthalpy through the change of local atomic movement from a smaller region

to a larger region. In another work, Qiao et al. [23] reported that the Fe addition into the ZrCuAlNi BMG led to decrement of Kohlrausch exponent and increase of characteristic relaxation time. Liu et al. [14] unveiled that the proper addition of Co and Cu into the LaCeAl glassy alloy intensified the secondary β relaxation and increased the glass transition temperature. The effects of Al and Nb microalloying process on the dynamic relaxation of $Zr_{20}Cu_{20}Ni_{20}Ti_{20}Hf_{20}$ high-entropy BMG were also evaluated through the mechanical spectroscopy [24]. The results unveiled that the activation energy of β relaxation for the Nb-added BMG was significantly higher, which was derived from the generation of severe chemical heterogeneity in the atomic structure. In another study, it was found that the Pd addition into the ZrCuAgAl BMG retarded the relaxation dynamics, which was indicative of defect-concentration reduction in the structure [25]. Previously, it was found that the Ni addition enhanced the total negative heat of mixing and changed the atomic arrangement and population of clusters in the ZrCoAl system, leading to the improvement of glass forming ability and structural heterogeneity [26]. Hence, it is concluded that the Ni element can be a proper minor addition for identification of dynamic response in the ZrCoAl MGs. In the current research, we aimed to focus on the characterization of dynamic relaxation evolution in a ZrCoAl BMG and indicate the importance of Ni microalloying process on the mechanical response of the glassy alloy in different conditions.

2. Experimental Procedure

In this study, $(Zr_{62}Co_{28}Al_{10})_{100\text{-}X}Ni_X$ (X = 0, 3 at.%) alloying compositions were considered for the fabrication. The negative heat of mixing for Ni-Al and Ni-Zr pairs is -22 kJ/mol and -49 kJ/mol [26], respectively, indicating that the Ni addition may improve the total heat of mixing and the structural disordering in the system. The mentioned alloys were firstly prepared by arc-melting process under the pure argon atmosphere. It should be noted that each master alloy was re-melted four times to obtain a homogenous chemical composition. Afterwards, the copper-mold suction casting was applied to fabricate BMGs in the form of plate samples with dimensions of 40 mm × 10 mm × 2 mm. To ensure the amorphousness of prepared samples, X-ray diffraction (XRD-Ultima IV) analysis was carried out at room temperature in the range of $2\theta = 25–90^{\circ}$. To characterize the thermal features of samples, the differential scanning calorimetry (DSC, TA instruments, 2500) was conducted under a high-purity dry argon environment with heating/cooling rates of 20 K/min. The measurement of relaxation enthalpy was carried out through the heating of sample beyond the glass transition temperature. After that a cooling process was performed to the room temperature. This cooling process was followed by a reheating stage with the identical heating rate. By subtracting the first and second thermal curves, the relaxation region is detected, which is consistent with the enthalpy of relaxation for samples. The dynamic mechanical analysis (DMA-Q800) was also performed in order to study the mechanical relaxation behavior of BMGs as function of frequency and temperature. This experiment was done under a protective atmosphere and different frequency and temperature ranges. From the attained data, the important parameters such as loss modulus (E″) and storage modulus (E′) were calculated [27]. The loss modulus is a criterion for evaluation of energy dissipation in an elastic excitation, while storage modulus is indicative of material ability to store energy elastically [28].

3. Results and Discussion

Figure 1(a) represents the XRD patterns of ZrCoAl and ZrCoAlNi samples with $2\theta = 25–90^{\circ}$. The results indicated that the XRD patterns included a broad peak with a smooth shoulder, implying the amorphous nature of samples. The DSC curves of samples are also given in Figure 1(b). As observed, the supercooled liquid range ($\Delta T_x = T_x - T_g$) in the ZrCoAl and Ni-added samples is 24 K and 32 K, respectively. The supercooled liquid range is a criterion for thermal stability and shows how easily a glassy alloy can be obtained after solidification. The enthalpy of relaxation is measured about 0.43 kJ/mol and 0.48 kJ/mol for the ZrCoAl and Ni-added samples, respectively. It is concluded that the minor Ni addition not only improves the thermal stability and glass formation but also is a key factor for the enhancement of stored energy in the atomic structure.

To characterize the relaxation processes, the dynamic mechanical response of samples was measured in a wide range of temperature under the heating rate of 5 K/min and driving frequency of 1 Hz. Figure 2(a) represents the normalized E'' and E' values for the ZrCoAl sample, while the loss factor ($\tan\delta = E''/E'$) for both of BMGs is given in Figure 2(b). According to the results, three distinct regions can be detected in the mechanical relaxation curve of ZrCoAl sample. At the first region (300 K–600 K), the loss modulus is low while the storage modulus is in its maximum state. In the temperature range of 600 K–730 K, the loss and storage moduli show the sharp increasing and decreasing trends, respectively. This event is associated to the β and α relaxations, occurring under the glass transition temperature [29, 30]. Finally, the contradictory behavior of moduli above 770 K is correlated to the nucleation and growth of crystals in the microstructure [25]. Using loss factor, it is possible to find out how the Ni microalloying process can change the relaxation behavior of ZrCoAl BMG. As given in Figure 2(b), the minor Ni addition leads to intensification of loss factor; however, a shift is detected in the peak of loss factor to the higher temperature, which is consistent with the DSC results in which the exothermic peak moves to the higher temperature for the Ni-added sample. There are also some published works showing the effects of minor addition on the deferment and intensification of relaxations in the glassy structures [9, 23, 31]. The intensification of relaxation is due to the increase of atomic mobility and free volumes.

The evaluation of mechanical relaxation on the different driving frequencies also gives important information about the activation energy of relaxation processes in the samples. As illustrated in Figure 3, the rise in the driving frequency leads to the shift of α-relaxation peak to the higher

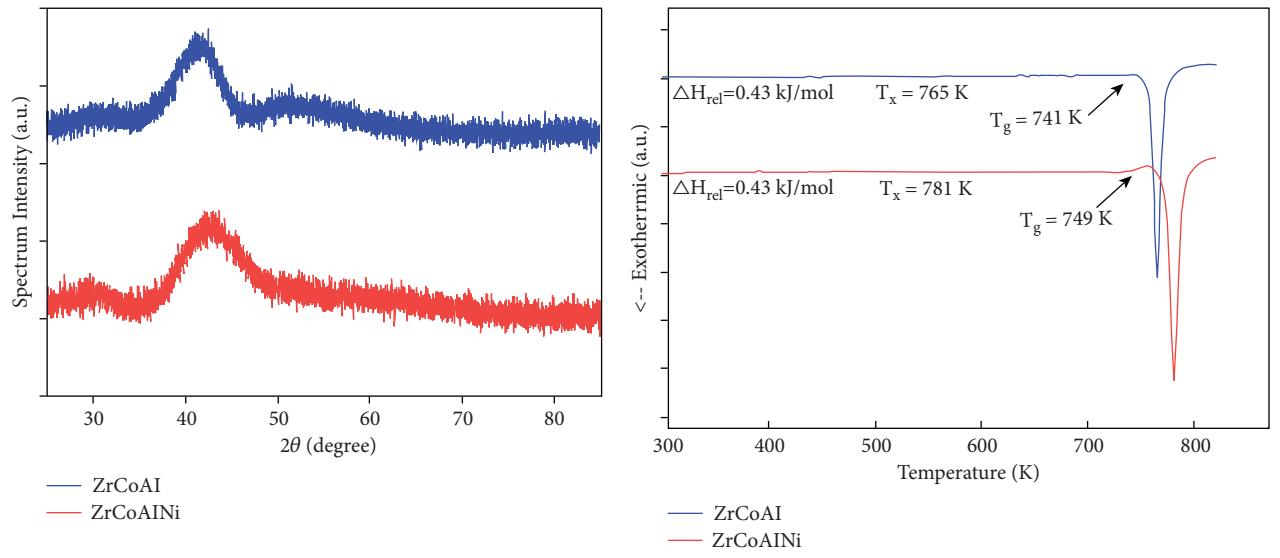

Figure 1: (a) XRD spectra and (b) DSC curves for ZrCoAl and ZrCoAlNi.

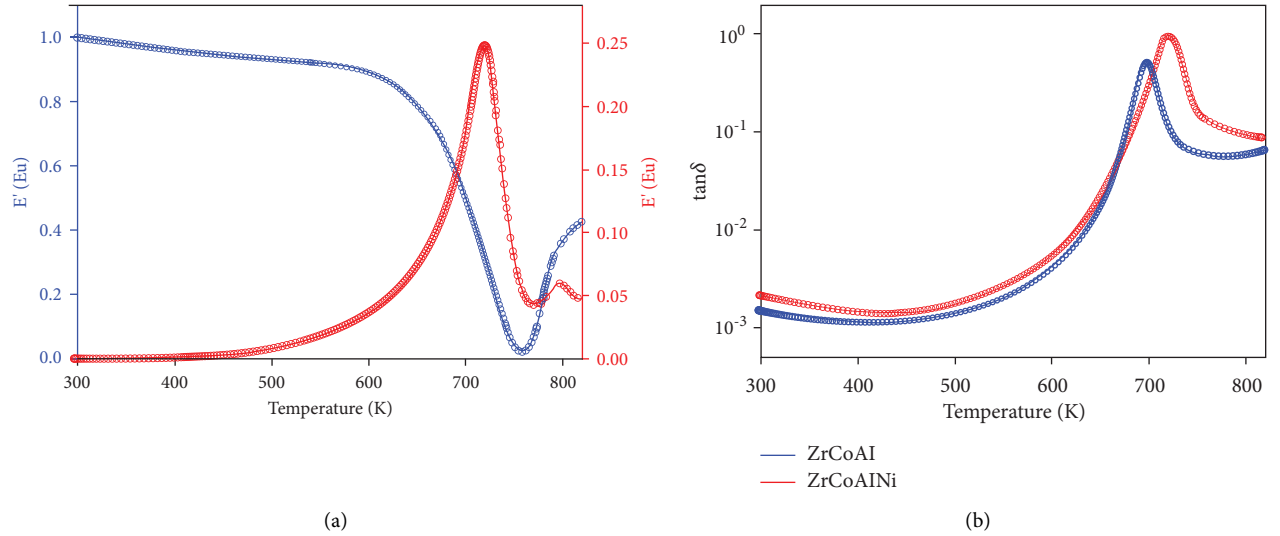

Figure 2: (a) Normalized E'' and E' values for the ZrCoAl sample. (b) Loss factor as a function of temperature for ZrCoAl and ZrCoAlNi.

temperatures for both samples; however, it is more pronounced in the ZrCoAlNi alloy. Using equation (1), it is feasible to calculate the activation energy of α relaxation [25]:

$$f = f_0 \exp\left(-\frac{E_a}{k_B}T\right), \tag{1}$$

in which the driving force and preexponential factor are introduced by f and f_0, respectively. Moreover, K_B and E_α define Boltzmann's constant and the activation energy of main relaxation in the system. As plotted in the insets, the fitted line of logarithm of frequency as a function of reciprocal of peak temperature represents the estimated value of activation energy for the BMGs. The estimations showed that the E_α value was 5.951 eV and 6.205 eV for ZrCoAl and ZrCoAlNi, respectively.

The physical aging below the glass transition temperature was also conducted to characterize the thermal features of samples. Figure 4 illustrates the normalized E' as a function of aging time under the driving frequency of 1 Hz for ZrCoAlNi BMG. Using equation (2), it is possible to describe the evolution of storage modulus in the system [32]:

$$\frac{E'(t)}{E_u} = \frac{A}{1+c},$$
$$c = \left(\frac{\tau_a}{\tau_b + t}\right)^{\beta_C}, \tag{2}$$

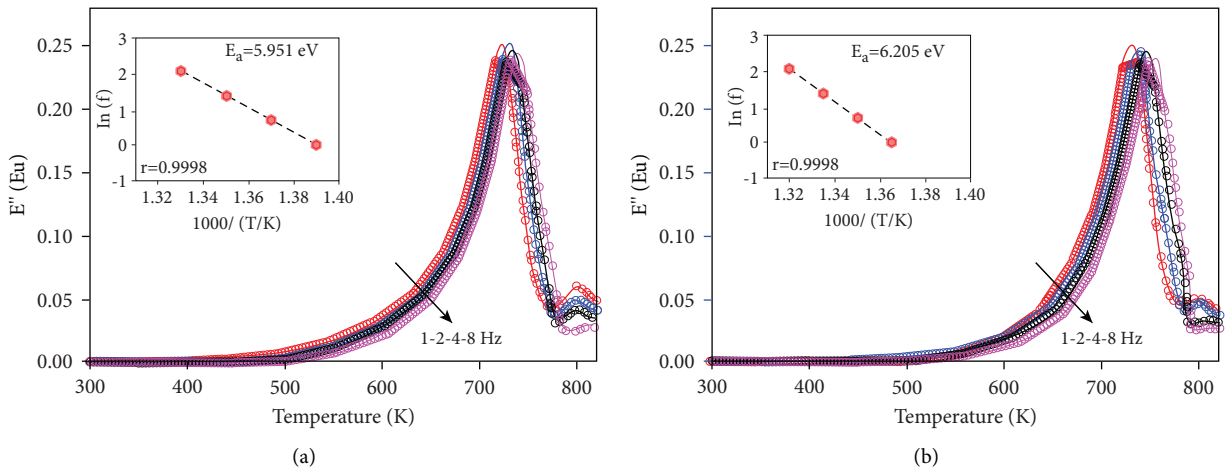

Figure 3: Temperature dependence of normalized loss modulus for different frequencies in (a) ZrCoAl and (b) ZrCoAlNi. The inset shows the estimation of activation energy by fitting driving frequency and temperature.

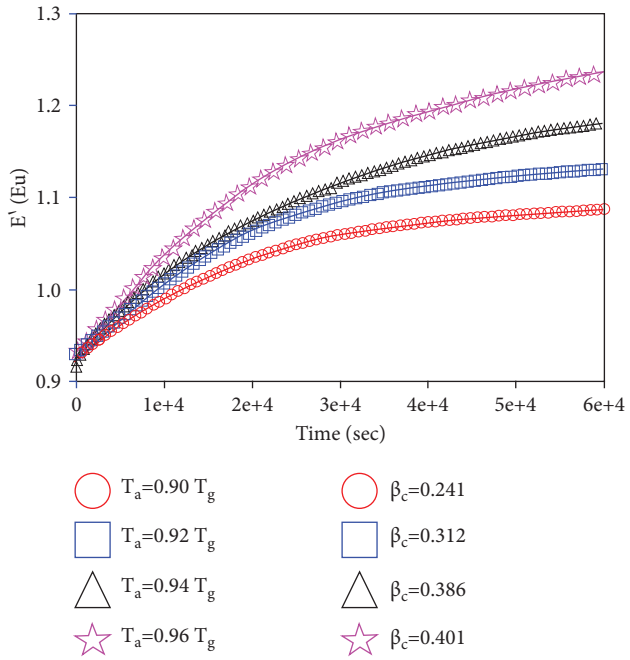

Figure 4: Normalized E' as a function of aging time under the driving frequency of 1 Hz for ZrCoAlNi BMG.

in which τ_a and τ_b are constants at the certain temperature and β_c is correlated to the rate of flow-unit annihilation in the aging process. The parameter "A" also introduces the normalized storage modulus in an infinite aging time. The results indicated that the β_c value is 0.241, 0.312, 0.386, and 0.401 at the annealing temperature of $0.90T_g$ $0.92T_g$, $0.94T_g$, and $0.96T_g$, respectively. Hence, it is concluded that the rise in annealing temperature accelerates the rate of flow-unit annihilation in the structure. Moreover, it is suggested that the sub-Tg annealing treatment stabilizes the amorphous structure at the lower energy levels without formation of any crystals in the material [33]. The Kohlrausch–Williams–Watts (KWW) function was applied to define the internal friction of BMGs [34]:

$$\tan\delta(t_a) - \tan\delta(t_a = 0) = A\left\{1 - \exp\left[-\left(\frac{t_a}{\tau}\right)^{\beta_{\text{aging}}}\right]\right\}, \quad (3)$$

where t_a introduces the aging time and β_{aging} is the KWW exponent describing the level of dynamic heterogeneity. β_{aging} parameter is in the range of 0-1, and it shows the intensified dynamic heterogeneity when it is in the minimum value [34]. The trends of tanδ as a function of annealing time with the driving force of 1 KHz for both samples are given in Figure 5. For ZrCoAlNi sample, β_{aging} declines with the rise of annealing temperature. On the other hand, ZrCoAl shows β_{aging} decreasing trend above the annealing temperature of $0.92T_g$. This means that both samples include a high dynamic heterogeneity at higher annealing temperatures. According to the previous works, β_{aging} dependency on the annealing temperature is different in the amorphous alloys [35, 36]. In addition to the chemical composition, it is strongly suggested that the initial energy state of alloys plays a crucial role in the improvement of dynamic heterogeneity at higher annealing temperatures [9]. In this work, it is also found that the minor Ni addition enhances the intensification of dynamic heterogeneity at high annealing temperature. As indicated in Figure 4, the initial state of storage modulus is in the same value for different annealing temperatures; however, it shows a temperature dependency with the increase of aging time. Moreover, the storage modulus is stabilized when the aging time exceeds from a certain value. On the other hand, Figure 5 indicates that the loss factor exhibited a decreasing trend with the rise of aging time. According to previous studies, the distribution of loosely and densely packed regions in the structure of amorphous alloys is responsible for the dynamic heterogeneity [37]. The loosely packed regions are also identified as the free volumes frozen under the quenching treatment [38]. These regions are potential sites for the generation of plastic deformation and can change the relaxation behavior of amorphous alloys [39]. The free volume also plays a significant role in the atomic mobility, elastic moduli, and mechanical properties of MGs [40].

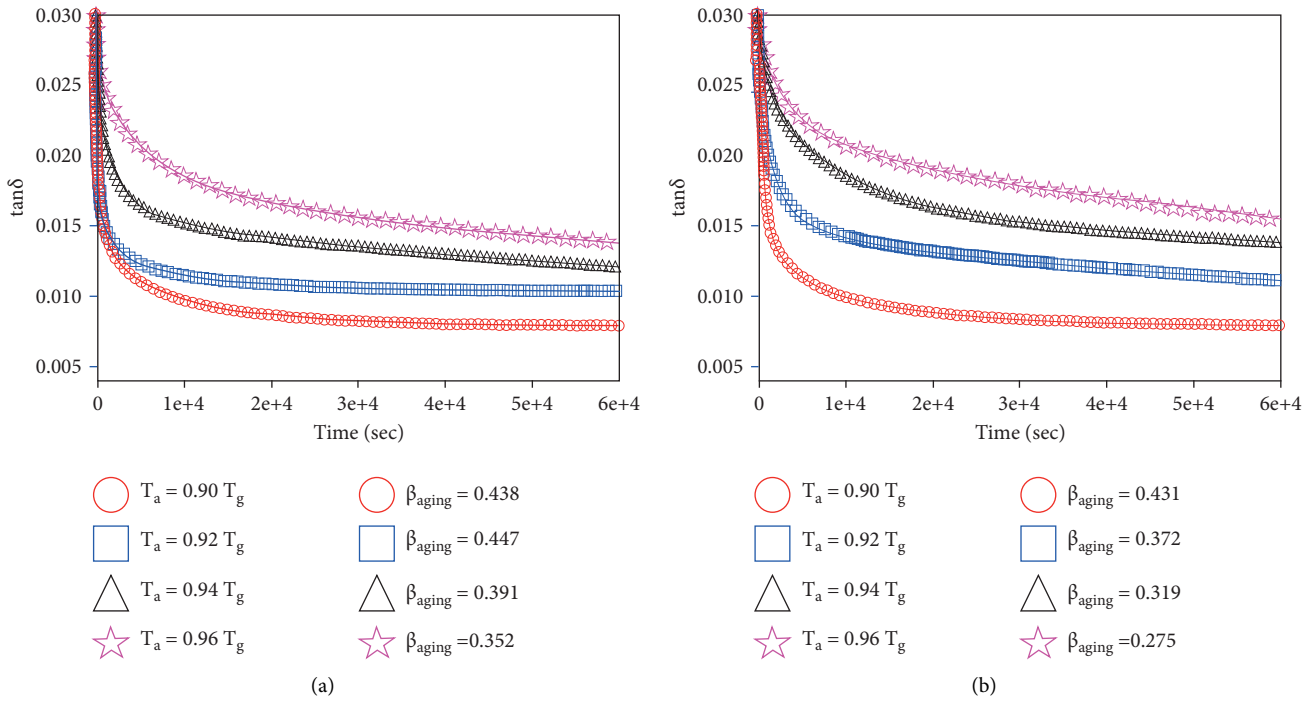

Figure 5: Loss factor as a function of aging time for (a) ZrCoAl and (b) ZrCoAlNi.

Based on Figures 4 and 5, the trends of loss factor and storage modulus of samples imply that the atomic mobility decreases at higher temperatures. Moreover, it is believed that with the increase of aging time, the free volumes are annihilated and the densely packed regions are prevailed in the system, leading to structural relaxation and increment of storage modulus; however, the material reaches an equilibrium state at long aging time, meaning that the rates of free volume annihilation and creation become identical.

The BMG samples were also evaluated through the isothermal frequency scanning method. Figures 6(a) and 6(b) illustrate the trend of normalized storage and loss moduli of ZrCoAlNi as a function of applied frequency. The results demonstrated that the decline of storage modulus is consistent with the decrease of frequency and increase of temperature, respectively. On the other hand, a peak is detected in the curves of loss modulus, shifting to the higher frequencies with the rise of temperature. It is believed that the peak is associated to α relaxation. An empirical function was also proposed by Williams and Watts [41] to characterize α relaxation in the amorphous systems:

$$E'(\omega) = \Delta E_a L_{i\omega}\left[-\frac{d\varphi_a(t,\tau_a)}{dt}\right]\varphi_a(t,\tau_a) = \exp\left[-\left(\frac{t}{\tau_a}\right)^{\beta_{KWW}}\right], \tag{4}$$

in which $L_{i\omega}$ and τ_α are Laplace transform and the primary relaxation time, respectively. ΔE_α introduces the relaxation strength and $\varphi\alpha$ $(t, \tau\alpha)$ is the empirical dielectric decay function. Moreover, another relaxation equation with few fitting parameters was proposed by Bergman [42]:

$$E''(\omega) = \frac{E_P}{\left\{1-\beta_{KWW}+\left(\beta_{KWW}/1+\beta_{KWW}\right)\left[\beta_{KWW}\left(\omega_P/\omega\right)+\left(\omega/\omega_P\right)^{\beta_{KWW}}\right]\right\}}, \tag{5}$$

where E_p and ω_p are normalized loss modulus and frequency at the potential peak (see Figure 7). As previously described, β_{KWW} is indicative of dynamic heterogeneity in the system so that with the increase of the exponent value from 0 to 1, the dynamic heterogeneity pales into insignificance in the microstructure. According to Figure 7, β_{KWW} values of the master curves for ZrCoAl and ZrCoAlNi are 0.502 and 0.493, respectively, showing the effects of Ni addition on the improvement of dynamic heterogeneity in the BMG. The figure also confirms that the experimental data are fitted by equation (5) at the peaks; however, there exist some deviations in the high-frequency part of the curves. Figure 7 also shows that the exponent is in the range of 0.5, as also reported in other works related to glassy alloys [43]. For

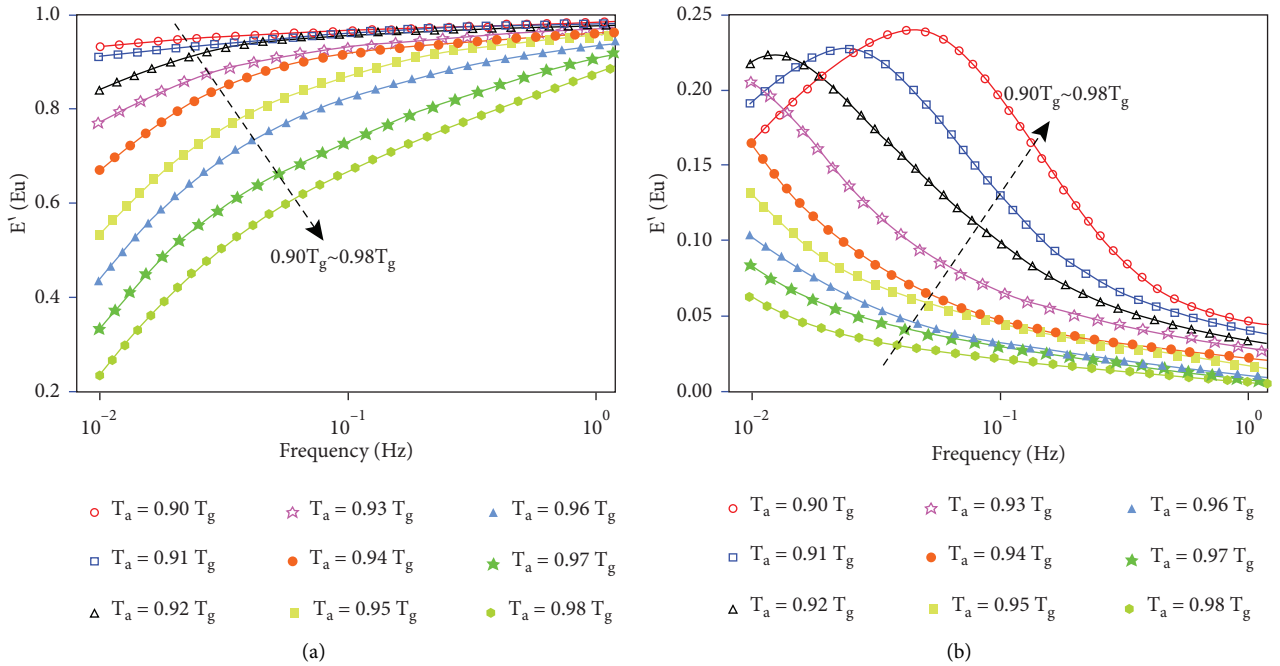

Figure 6: The trend of normalized (a) storage modulus and (b) loss modulus of ZrCoAlNi as a function of applied frequency.

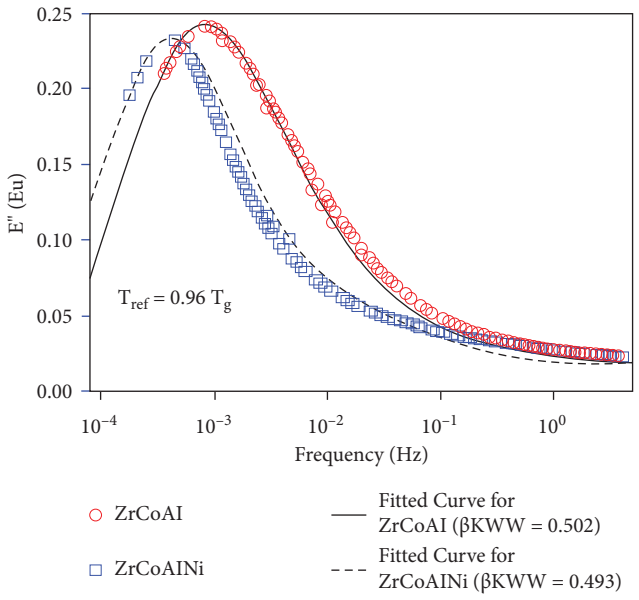

Figure 7: Master curves of ZrCoAl and ZrCoAlNi MGs fitted by the Bergman equation.

evaluation of dynamic mechanical behavior of MGs, it is also possible to apply the theory of quasi-point defects (QPDs) [44]. In this theory, the defect concentration of glassy structure is quantified and correlated to the normalized loss modulus:

$$E''(\omega) = \frac{E_u}{\left[1 + \lambda (i\omega\tau)^{-\chi} + (i\omega\tau)^{-1}\right]}. \quad (6)$$

By fitting the loss modulus-frequency curve, it is possible to obtain correlation factor (χ), numerical factor (λ), and global characteristics time (τ) for the samples. The correlation factor (χ) is indicative of concentration of quasi-point defects in the system and it stands between 0 and 1. At $\chi = 1$, the material shows the state of an ideal gas, while a perfect crystal has a minimum correlation factor ($\chi = 0$). Figure 8 shows the fitted data of loss modulus-frequency based on the QPD model. According to the results, the correlation factor is 0.417 and 0.431 for ZrCoAl and ZrCoAlNi samples, respectively. This means that the Ni addition may increase the defect concentration and lead to the rise of loss modulus in the glassy alloy, which is consistent with the data fitted by the Bergman equation (see Figure 7). In general, it is believed that the increase in dynamic heterogeneity is accompanied with the generation and distribution of loosely packed structure and intensifies the structural defects in the system. However, one should note that the rate of dynamic heterogeneity improvement and defect generation is not similar. As can be seen in Figure 9, the relative variation of β_{KWW} is sharper than χ parameter with the increase of temperature. This implies that it is possible to improve the dynamic heterogeneity through a small introduction of defects, i.e., free volumes, into the system. As a topological point of view, it was found that the Ni addition into the ZrCoAl MGs leads to the rise in types of atomic clusters, i.e., short range orders, stabilizing the liquid and glass formation [26]. However, one should note that the increase of cluster types is a main reason for generation of nanoscale defects in the structure, leading to the improvement of heterogeneity. This event was also reported in other works. For instance, the minor addition of Ni and Co in the LaGa-based MGs leads to the shift of relaxation peak to higher temperatures, while the

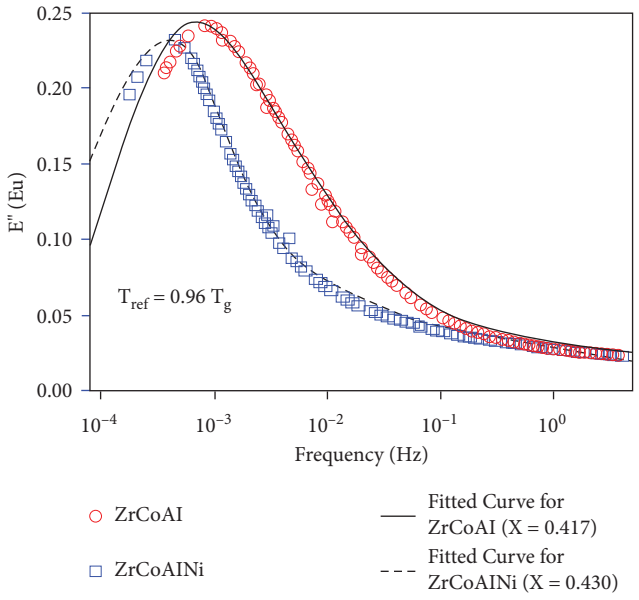

Figure 8: Master curves of ZrCoAl and ZrCoAlNi MGs fitted by the QPD equation.

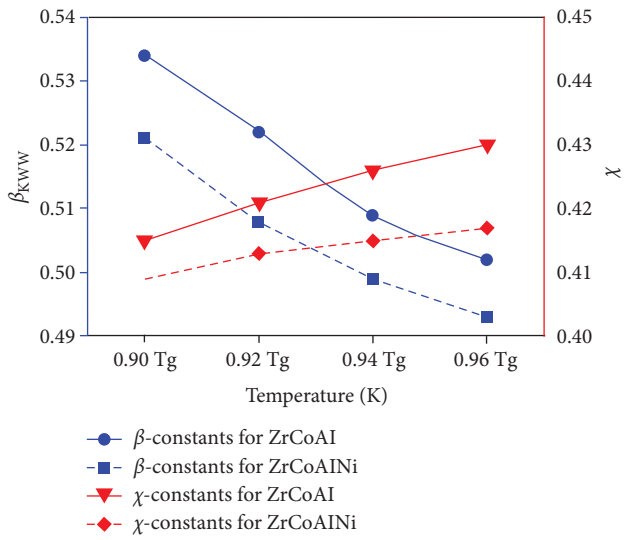

Figure 9: Variations of β_{KWW} and χ parameters as a function of temperature.

peak becomes more pronounced [45]. It was also reported that the minor Gd addition in the CuZr-based MG intensifies the boson peaks in the thermographs and improves the structural heterogeneity [46].

4. Conclusions

In this study, the mechanical relaxation behaviors of BMGs with alloying compositions of ZrCoAl and ZrCoAlNi were investigated in detail. The main outcomes are as follows:

(i) The minor Ni addition not only improved the thermal stability but also enhanced the enthalpy of relaxation. Moreover, it was found that the relaxation event was retarded in the Ni-added sample.

(ii) The DMA results indicated that the Ni addition generated the loosely packed structure and enhanced the dynamic heterogeneity in the amorphous alloy.

(iii) The fitted data of loss modulus-frequency based on the QPD model show that the correlation factor is 0.417 and 0.431 for ZrCoAl and ZrCoAlNi samples, respectively. This means that the Ni addition may increase the defect concentration and lead to the rise of loss modulus in the glassy alloy, which is consistent with that resulting from the KWW model.

Data Availability

The data used to support the findings of this study are included within the article.

Conflicts of Interest

The authors declare that they have no conflicts of interest.

References

[1] M. Li, H. Guan, S. Yang, X. Ma, and Q. Li, "Minor Cr alloyed Fe–Co–Ni–P–B high entropy bulk metallic glass with excellent mechanical properties," *Mater. Sci. Eng*, vol. 805, 2020.

[2] Z. Li, M. Zhang, J. Wang, N. Li, and L. Liu, "Pronounced softening of a Zr-based metallic glass in micro annular gap flow," *Materials Research Letters*, vol. 10, no. 2, pp. 62–69, 2022.

[3] M. Shi, J. Chen, and C. Chen, "Inverse size effects in unnotched and notched metallic glass thin films," *Journal of Non-crystalline Solids*, vol. 575, Article ID 121172, 2022.

[4] P. Sonia and S. Kumari, "Performance evaluation of multifibre (hybrid) polymer composite," *IOP Conference Series: Materials Science and Engineering*, vol. 1116, no. 1, Article ID 012027, 2021.

[5] L. T. Zhang, Y. J. Wang, E. Pineda, H. Kato, Y. Yang, and J. C. Qiao, "Sluggish dynamics of homogeneous flow in high-entropy metallic glasses," *Scripta Materialia*, vol. 214, Article ID 114673, 2022.

[6] S. Zhang, W. Wang, and P. Guan, "Dynamic crossover in metallic glass nanoparticles," *Chinese Physics Letters*, vol. 38, no. 1, Article ID 016802, 2021.

[7] D. Bandhu, J. J. Vora, S. Das et al., "Experimental study on application of gas metal arc welding based regulated metal deposition technique for low alloy steel," *Materials and Manufacturing Processes*, pp. 1–19, 2022.

[8] S. Kumari, B. Nakum, D. Bandhu, and K. Abhishek, "Multi-attribute group decision making (MAGDM) using fuzzy linguistic modeling integrated with the VIKOR method for car purchasing model," *International Journal of Decision Support System Technology*, vol. 14, pp. 1–20, 2022.

[9] W. H. Wang, "Dynamic relaxations and relaxation-property relationships in metallic glasses," *Progress in Materials Science*, vol. 106, Article ID 100561, 2019.

[10] Q. Hao, W. Y. Jia, and J. C. Qiao, "Dynamic mechanical relaxation in Zr65Ni7Cu18Al10 metallic glass," *Journal of Non-crystalline Solids*, vol. 546, Article ID 120266, 2020.

[11] G. J. Lyu, J. C. Qiao, J.-M. Pelletier, and Y. Yao, "The dynamic mechanical characteristics of Zr-based bulk metallic glasses and composites," *Materials Science and Engineering A*, vol. 711, pp. 356–363, 2018.

[12] D. R. Tripathi, K. H. Vachhani, D. Bandhu, S. Kumari, V. R. Kumar, and K. Abhishek, "Experimental investigation and optimization of abrasive waterjet machining parameters for GFRP composites using metaphor-less algorithms," *Materials and Manufacturing Processes*, vol. 36, no. 7, pp. 803–813, 2021.

[13] L. Zhang, Y. Duan, D. Crespo et al., "Dynamic mechanical relaxation and thermal creep of high-entropy La30Ce30-Ni10Al20Co10 bulk metallic glass," *Science China Physics, Mechanics & Astronomy*, vol. 64, no. 9, Article ID 296111, 2021.

[14] M. Liu, J. Qiao, Q. Hao et al., "Dynamic mechanical relaxation in LaCe-based metallic glasses: Influence of the chemical composition," *Metals*, vol. 9, p. 1013, 2019.

[15] K. Tao, J. C. Qiao, Q. F. He, K. K. Song, and Y. Yang, "Revealing the structural heterogeneity of metallic glass: mechanical spectroscopy and nanoindentation experiments," *International Journal of Mechanical Sciences*, vol. 201, Article ID 106469, 2021.

[16] A. Das, E. M. Dufresne, and R. Maaß, "Structural dynamics and rejuvenation during cryogenic cycling in a Zr-based metallic glass," *Acta Materialia*, vol. 196, pp. 723–732, 2020.

[17] T. Pérez-Castañeda, C. Rodríguez-Tinoco, J. Rodríguez-Viejo, and M. A. Ramos, "Suppression of tunneling two-level systems in ultrastable glasses of indomethacin," *Proceedings of the National Academy of Sciences*, vol. 111, no. 31, pp. 11275–11280, 2014.

[18] J. C. Qiao, Y. Yao, J. M. Pelletier, and L. M. Keer, "Understanding of micro-alloying on plasticity in Cu46Zr47−xAl7Dyx (0≤ x ≤ 8) bulk metallic glasses under compression: based on mechanical relaxations and theoretical analysis," *International Journal of Plasticity*, vol. 82, pp. 62–75, 2016.

[19] G. R. Garrett, M. D. Demetriou, J. Chen, and W. L. Johnson, "Effect of microalloying on the toughness of metallic glasses," *Applied Physics Letters*, vol. 101, no. 24, Article ID 241913, 2012.

[20] K. Tao, J. C. Qiao, L. Zhang, and J. M. Pelletier, "Dynamic mechanical response of ZrCu-based bulk metallic glasses," *International Journal of Mechanical Sciences*, vol. 211, Article ID 106770, 2021.

[21] I. Raya, T.-C. Chen, S. H. Pranoto et al., "Role of Si minor addition on glass formation and flow stress characteristics of a Zr-based metallic glass," *Materials Research*, vol. 24, no. 6, 2021.

[22] L. Xu, Q. Lu, and Q. Zhang, "Effects of refractory Nb on glass-forming ability and structure inhomogeneity of Cu50Zr50 binary metallic glass," *Materials Research Express*, vol. 6, no. 9, Article ID 095203, 2019.

[23] J. C. Qiao, J. Cong, Q. Wang, J. M. Pelletier, and Y. Yao, "Effects of iron addition on the dynamic mechanical relaxation of Zr55Cu30Ni5Al10 bulk metallic glasses," *Journal of Alloys and Compounds*, vol. 749, pp. 262–267, 2018.

[24] D. Li, C. Jiang, H. Li, and M. Pandey, "Crystallization evolution and relaxation behavior of high entropy bulk metallic glasses using microalloying process," *Chinese Physics B*, vol. 30, no. 6, Article ID 066401, 2021.

[25] Y. T. Cheng, Q. Hao, J. C. Qiao, D. Crespo, E. Pineda, and J. M. Pelletier, "Effect of minor addition on dynamic mechanical relaxation in ZrCu-based metallic glasses," *Journal of Non-crystalline Solids*, vol. 553, Article ID 120496, 2021.

[26] M. Samavatian, R. Gholamipour, and V. Samavatian, "Discovery of novel quaternary bulk metallic glasses using a developed correlation-based neural network approach," *Computational Materials Science*, vol. 186, Article ID 110025, 2021.

[27] Q. Wang, S. T. Zhang, Y. Yang, Y. D. Dong, C. T. Liu, and J. Lu, "Unusual fast secondary relaxation in metallic glass," *Nature Communications*, vol. 6, no. 1, p. 7876, 2015.

[28] J. D. Ju and M. Atzmon, "A comprehensive atomistic analysis of the experimental dynamic-mechanical response of a metallic glass," *Acta Materialia*, vol. 74, pp. 183–188, 2014.

[29] L. T. Zhang, Y. J. Duan, T. Wada et al., "Dynamic mechanical relaxation behavior of Zr35Hf17. 5Ti5. 5Al12. 5Co7. 5Ni12Cu10 high entropy bulk metallic glass," *Journal of Materials Science & Technology*, vol. 83, pp. 248–255, 2021.

[30] X. Cui, J. Guo, J. c Qiao et al., "Influence of the chemical composition on the β-relaxation and the mechanical behavior of LaCe-based bulk metallic glasses," *Journal of Non-crystalline Solids*, vol. 562, Article ID 120779, 2021.

[31] S. H. Xie, X. R. Zeng, and H. X. Qian, "Correlations between the relaxed excess free volume and the plasticity in Zr-based bulk metallic glasses," *Journal of Alloys and Compounds*, vol. 480, no. 2, pp. L37–L40, 2009.

[32] D. P. Wang, Z. G. Zhu, R. J. Xue, D. W. Ding, H. Y. Bai, and W. H. Wang, "Structural perspectives on the elastic and mechanical properties of metallic glasses," *Journal of Applied Physics*, vol. 114, no. 17, Article ID 173505, 2013.

[33] J. W. Lv, D. W. Yin, F. L. Wang, Y. J. Yang, M. Z. Ma, and X. Y. Zhang, "Influence of sub-Tg annealing on microstructure and crystallization behavior of TiZr-based bulk metallic glass," *Journal of Non-crystalline Solids*, vol. 565, Article ID 120855, 2021.

[34] J. C. Qiao and J. M. Pelletier, "Dynamic mechanical relaxation in bulk metallic glasses: a review," *Journal of Materials Science & Technology*, vol. 30, no. 6, pp. 523–545, 2014.

[35] A. Ishii, "Spatial and temporal heterogeneity of Kohlrausch–Williams–Watts stress relaxations in metallic glasses," *Computational Materials Science*, vol. 198, Article ID 110673, 2021.

[36] W. Zhai, C. H. Wang, J. C. Qiao, J.-M. Pelletier, F. P. Dai, and B. Wei, "Distinctive slow β relaxation and structural heterogeneity in (LaCe)-based metallic glass," *Journal of Alloys and Compounds*, vol. 742, pp. 536–541, 2018.

[37] J.-L. Gu, H.-W. Luan, S.-F. Zhao et al., "Unique energy-storage behavior related to structural heterogeneity in high-entropy metallic glass," *Materials Science and Engineering A*, vol. 786, Article ID 139417, 2020.

[38] F. Zhu, S. Song, K. M. Reddy, A. Hirata, and M. Chen, "Spatial heterogeneity as the structure feature for structure–property relationship of metallic glasses," *Nature Communications*, vol. 9, no. 1, p. 3965, 2018.

[39] C. Ma, S. Suslov, C. Ye, and Y. Dong, "Improving plasticity of metallic glass by electropulsing-assisted surface severe plastic deformation," *Materials & Design*, vol. 165, Article ID 107581, 2019.

[40] W. Guo, R. Yamada, and J. Saida, "Rejuvenation and Plasticization of Metallic Glass by Deep Cryogenic Cycling Treatment," *Intermetallics*, vol. 93, pp. 141–147, 2018.

[41] G. Williams and D. C. Watts, "Non-symmetrical dielectric relaxation behaviour arising from a simple empirical decay function," *Transactions of the Faraday Society*, vol. 66, p. 80, 1970.

[42] R. Bergman, "General susceptibility functions for relaxations in disordered systems," *Journal of Applied Physics*, vol. 88, no. 3, pp. 1356–1365, 2000.

[43] J. C. Qiao and J. M. Pelletier, "Kinetics of structural relaxation in bulk metallic glasses by mechanical spectroscopy:

determination of the stretching parameter βKWW," *Intermetallics*, vol. 28, pp. 40–44, 2012.

[44] J. C. Qiao, Y. X. Chen, J.-M. Pelletier et al., "Viscoelasticity of Cu-and La-based bulk metallic glasses: interpretation based on the quasi-point defects theory," *Materials Science and Engineering A*, vol. 719, pp. 164–170, 2018.

[45] R. J. Xue, L. Z. Zhao, B. Zhang, H. Y. Bai, W. H. Wang, and M. X. Pan, "Role of low melting point element Ga in pronounced β-relaxation behaviors in LaGa-based metallic glasses," *Applied Physics Letters*, vol. 107, no. 24, Article ID 241902, 2015.

[46] Y. Li, H. Y. Bai, W. H. Wang, and K. Samwer, "Low-temperature specific-heat anomalies associated with the boson peak in CuZr-based bulk metallic glasses," *Physical Review B: Condensed Matter*, vol. 74, no. 5, Article ID 052201, 2006.